sustainability

Article

Experimental Study on Flexural Performance of Regulated Reinforced Glulam Beam after Long-Term Loading

Nan Guo [1], Chao Yang [1], Ling Li [1,*], Guodong Li [1] and Yan Zhao [2]

[1] College of Civil Engineering, Northeast Forestry University, Harbin 150040, China; snowguonan@163.com (N.G.); yangchaoedc@163.com (C.Y.); ldlgd@163.com (G.L.)
[2] School of Civil Engineering and Architecture, Wuyi University, Wuyishan 354300, China; zhaoyan_hit@163.com
* Correspondence: liling0048hit@163.com

Abstract: Due to wood creep characteristics, the failure mode, bearing capacity, stiffness, and deformation of its components are doomed to be impacted by long-term loading. This paper conducted a comparative test on creep beams, regulated beams, and short-term beams based on the former long-term loading research. The results demonstrated that the glulam beam experienced tensile failure of the beam-bottom, while the horizontal joint failure and the local compressive failure of the beam-end happened in the reinforced glulam beam and the prestressed glulam beam. The bearing capacity of the creep beams decreased compared with that of the short-term beams; the decline in the bearing capacity of the ordinary glulam beams, the reinforced glulam beams, and the prestressed glulam beams ranged from 3.2% to 9.8%, from 1.6% to 13.2%, and from 2.9% to 9.2%, respectively. However, the bearing capacity of the regulated beam with the deformation restored to the initial value of the load increased by 4.6–14.1%. The prestressed regulation changed the distribution of the stress on the beam and thus enhanced its bearing capacity. The findings of this work could be used as a frame of reference for similar components in engineering applications.

Keywords: reinforced glulam beams; flexural performance; bearing capacity; creep; prestressed control

check for updates

Citation: Guo, N.; Yang, C.; Li, L.; Li, G.; Zhao, Y. Experimental Study on Flexural Performance of Regulated Reinforced Glulam Beam after Long-Term Loading. *Sustainability* **2021**, *13*, 5556. https://doi.org/10.3390/su13105556

Academic Editors: Edwin B. Zea Escamilla and David Trujillo

Received: 18 March 2021
Accepted: 30 April 2021
Published: 17 May 2021

1. Introduction

In recent years, wood structures have been paid extensive attention to and actively promoted due to their characteristics of environmental protection and sustainable development [1–6]. Glulam is an important material of wooden structures, which has several advantages such as scattered defects, high strength, and variable shapes of cross-sections and components, etc. [7–9]. However, glulam beams are prone to brittle tensile failure under bending, and the creep characteristics of the wood, which with the majority of compressive strength of wood, are not fully utilized. The work proposed a type of composite member which was slotted at the lower part of the glulam beam to configure a steel bar; then, the steel bar was tensioned, and the glulam was compressed, that is, a regulated reinforced glulam beam was produced [10–13]. This form of beam was endowed with the better compressive strength of glulam; thus, the beam could enjoy the plastic compression failure of glulam, and its deformation could be reduced by regulating the prestress magnitude in service. Therefore, the creep effect was reduced. It is well known that creep is one of the basic characteristics of wood, which increases the long-term deformation of wood components and reduces its strength and stiffness to a certain extent. Such characteristics can take a toll on the safety performance of structures [14–17]. Therefore, studying the flexural performance of regulated reinforced glulam beams after long-term loading has important research value and engineering significance.

In recent years, related domestic and foreign research mainly focused on aspects such as creep characteristics of wood, creep of components and structures [18–20], mechanical properties of glulam beams, etc. [21–25]. There were few studies on the flexural performance of the glulam beam after long-term loading, and this reinforced glulam beam was a new type of component proposed by the project team. Therefore, there was no related research; however, previous research and related results could provide references for this article.

This paper presented a short-term loading failure test that was performed on the glulam beam after long-term loading analyzing the failure mode, bearing capacity, and deformation, etc. To conduct a comparative test on creep beams, regulated beams, and short-term beams, our research group evaluated the influence of glulam creep and reinforcement regulation on beam performance.

2. Materials and Methods

2.1. Composition of the Regulated Reinforced Glulam Beam

According to relevant standards [26,27], the test beams in this paper, with a size of 3100 mm × 150 mm × 100 mm, were designed and fabricated, and the regulated reinforced glulam beams included glulam beams, steel bars, and tension anchorage devices at the end, as shown in Figure 1. Two grooves with the dimensions 22 mm × 30 mm were set up at the bottom of the glulam beam 15 mm away from the two sides of the beam. The reinforcement was placed in the groove, and the end was anchored through an anchor plate set at the end of the beam. The beam section is displayed in Figure 2. A thread was formed at the end of the steel bar, and the prestress could be applied by tightening the screw cap at the end, thereby forming a regulated reinforced glulam beam with a simple structure and reasonable force. The strain gauge was pasted to the middle of the steel bar, and the measured strain values of the test process were monitored in real-time; the prestress was also regulated precisely.

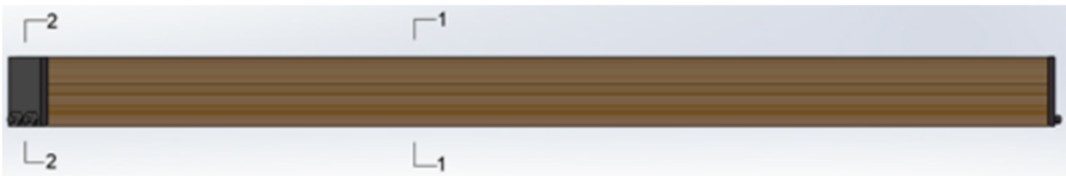

Figure 1. Reinforced glulam beam elevation view.

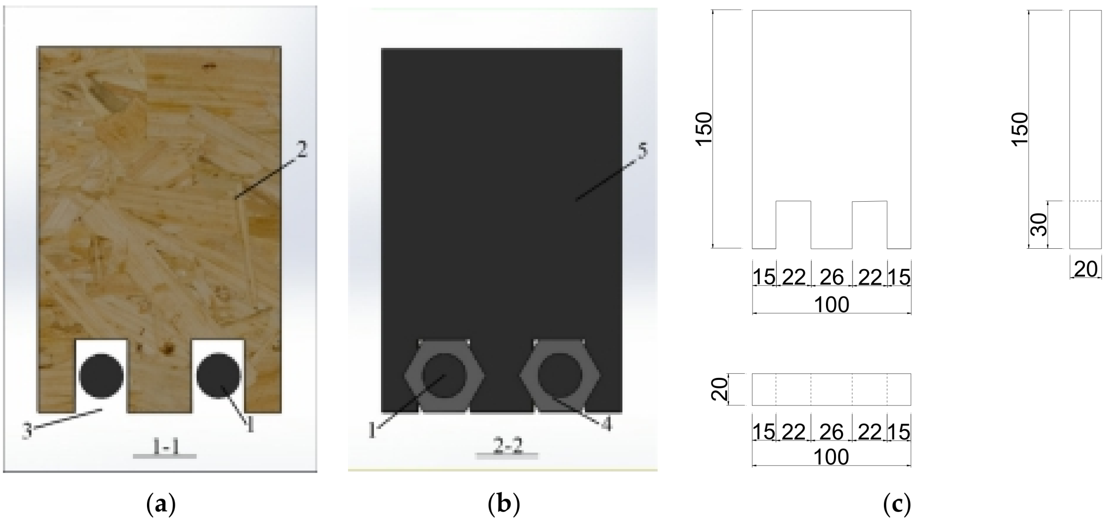

Figure 2. Reinforced glulam beam sectional view. (**a**) Sectional view of 1–1; (**b**) sectional view of 2–2. 1. steel bar; 2. glulam; 3. groove; 4. nut; 5. anchor bearing plate; (**c**) steel plate processing view.

Regulated reinforced glulam beams were produced, Pinus sylvestris were used as the raw material of glulam, and HRB400 steel bars were used as the tensile steel bars for the glulam beam. The physical and mechanical properties of the glulam and the steel bar are shown in Tables 1 and 2, respectively.

Table 1. Mechanical properties of glulam.

Material	Average Tensile Strength (MPa)	Design Tensile Strength MPa)	Average Compressive Strength (MPa)	Design Compressive Strength (MPa)	Elastic modulus (N/mm^2)
Pinus sylvestris	66.5	10.51	36.62	14.68	8515.75

Table 2. Mechanical parameters of steel.

Diameter (mm)	Yield Strength F_y (MPa)	Ultimate Strength F_u (MPa)	Elastic Modulus E_y (N/mm^2)
14	428	573	2.01×10^5
16	434	586	2.01×10^5
18	441	601	2.01×10^5

2.2. Experimental Method

The short-term loading test of glulam beams was conducted after the 90-day long-term loading test. During the 90-day long-term loading test, the temperature and humidity of the test beam were regularly monitored. The data obtained showed that, although the external environment changed significantly, the temperature of the laboratory was maintained at (20 ± 3) °C and the relative humidity was maintained at (70 ± 5)%, and it generally changed little. The influence of temperature and humidity on the analysis of the test results could be ignored. When conducting a long-term test, according to beam type, loading level, reinforcement ratio, and total prestress level, the test pieces were divided into four groups A, B, C, and D, as shown in Table 3. Inside:

Groups A and B: glulam beams and reinforced glulam beams. The loading level was the variable;
Group C: reinforced glulam beams to which the same external load was applied, and the variable was the reinforcement ratio;
Group D: prestressed glulam beams to which the same external load and the reinforcement ratio were applied, and the variable was the prestress value.

After 90 days of the long-term test, the failure analysis of the beams was carried out in the shortest time. Out of the two groups C and D, under working conditions, one was directly loaded to evaluate the influence of creep on the failure mode, bearing capacity, and deflection of the beam, and the other was prestressed to restore the midspan deflection to the initial elastic deflection value for the purpose of examining the regulation effect on the beam. For convenience, the beams directly subjected to short-term loading after long-term loading were referred to as creep beams, and the beams subjected to short-term loading after long-term loading were referred and then regulated to become regulated beams.

According to the relevant standards [26,27], the four-point bending test was employed in this test, and a loading system adopted loading control and displacement control [2]. In the early stage of loading, force control was adopted, and the load of each stage was taken as 10% of the predicted ultimate load. After reaching 50% of the predicted ultimate load, the load of each stage was reduced to 5% of the predicted ultimate load; when the loading value equaled 80% of the predicted ultimate load, the displacement control was used, the midspan deflection was recorded as ω_0, which increased gradually by $0.05\omega_0$ per stage until the test beam was destroyed.

Table 3. Test matrix.

Group	Number of the Component	Loading Level	Load Value (kN)	Reinforcement Ratio [2] (%)	Prestress Value (MPa)
A (L_A)	L_{A1}	20%	4.66	0	0
	L_{A2}	30%	6.99	0	0
	L_{A3}	40%	9.32	0	0
B (PL_B)	PL_{B1}	20%	6.18	3.39	0
	PL_{B2} [1]	30%	9.12	3.39	0
	PL_{B3}	40%	12.36	3.39	0
C (PL_C)	PL_{C1-1} [1]	30%	9.12	3.39	0
	PL_{C1-2}	30%	9.12	3.39	0
	PL_{C2-1}	30%	9.09	2.68	0
	PL_{C2-2}	30%	9.09	2.68	0
	PL_{C3-1}	30%	9.00	2.05	0
	PL_{C3-2}	30%	9.00	2.05	0
D (YL_D)	YL_{D1-1}	30%	9.18	3.39	30
	YL_{D1-2}	30%	9.18	3.39	30
	YL_{D2-1}	30%	10.05	3.39	60
	YL_{D2-2}	30%	10.05	3.39	60

[1] In the table, the PL_{B2} and PL_{C1-1} were exactly the same and had different numbers due to different groups; [2] The reinforcement ratio is the ratio of the area of reinforcement to the area of beam section.

To measure the uneven settlement the of the bracket and the mid-span deflection of the beams, a displacement meter with a range of 50 mm was attached to the bracket and at the third point at both ends of the beam, and a displacement meter with a range of 200 mm was installed at the midspan of the beam.

The strain of glulam and steel bars was measured with strain gauges. Six strain gauges were uniformly pasted along the side surface at three equal points on both sides of the glulam beam. Moreover, two strain gauges were attached to the top and bottom surfaces of the beam mid-span, respectively. As for the reinforced glulam beams, one strain gauge was attached to the middle position of two steel bars at the groove of the beam-bottom, as shown in Figure 3. During the loading process, at the end and mid-span of the beam the deflection changed; bar wire and glulam beam stress changes were all synchronously collected by the Model JM3813 multifunctional static strain test system.

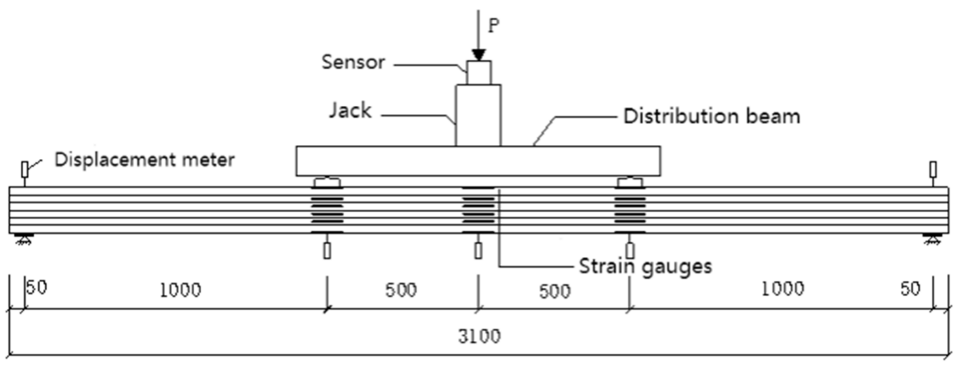

Figure 3. Loading device.

3. Results

According to the test results, the failure types of glulam beams were classified into three types of destruction, including the tensile failure of the beam-bottom, the horizontal joint failure, and the local compressive failure of the beam-end.

3.1. The Tensile Failure of the Beam-Bottom

This type of failure was chiefly manifested as the formation of cracks at the defects, such as the beam-bottom joint at the beginning of the loading. With the increase in the load, the deflection rose correspondingly. The bottom plate of the glulam was then ruptured, which eventually descended the bearing capacity of the beam; thus, a brittle failure was induced, as shown in Figure 4.

Figure 4. Status of the tensile failure of the beam-bottom.

3.2. The Horizontal Joint Failure

The failure mode mainly occurred in the loading process: the wood joints in the middle of the beam height at the third point were first cracked, and a slight horizontal crack was formed. With the increase in the load, the crack gradually extended to the end of the beam. Due to the tensile force in the reinforcement, the anchor plate at the end of the beam was warped, and, finally, the shear failure along the grain occurred. It should be noted that when the span-to-depth ratio was greater than 10, the glulam beam generally suffered from bending failure rather than shear failure. However, due to the defects in the middle of the beam height and the presence of the reinforcement and the anchor plate at the end of the beam, the longitudinal shear force in the beam increased, so the longitudinal shear failure happened, which was manifested as the horizontal joint failure, as shown in Figure 5.

Figure 5. Status of the horizontal joint failure.

3.3. The Local Compressive Failure of the Beam-End

In the third type of failure, the first cracking occurred at the defect in the beam-bottom, and then the bottom plate was ruptured. As the load enlarged, the fracture surface continued to grow upward, resulting in wrinkles in the top layer of the glulam. In this process, the tensile force of the steel bar increased, but the bearing capacity of the end of the beam was reduced by setting the groove. Finally, a local compressive failure at the end of the beam occurred, as shown in Figure 6.

(a)

(b)

Figure 6. Status of the local compressive failure. (**a**) At the top of beam is folded; (**b**) the anchor plate is warped.

3.4. Classification and Analysis of Failure Modes

On performing statistical analysis on the test results of the glulam beams and the creep beams, the results demonstrated that the ordinary glulam beam experienced the tensile failure at the bottom of the beam, while the horizontal joint failure and the local compressive failure of the beam-end happened in the reinforced glulam beam and the prestressed glulam beam. The reason was the tensile force of the steel bars, which led to the change of the failure form; however, the failure form depended on the glulam timber parallel-to-grain shear strength and the beam-end parallel-to-grain and compression strength. If the parallel-to-grain shear strength was higher than the latter, local compressive failure of the beam-end occurred, otherwise, horizontal joint failure occurred; in the reinforced glulam beam and prestressed glulam beam also horizontal joint failure of the beam-end and the local compressive failure occurred, due to the same reason as above. The specific failure modes are shown in Table 4, and the distribution of the failure mode is shown in Figure 7.

Table 4. Information of failure modes of glulam beams.

Group	Number of the Component	Failure Modes
Creep beams	L_{A1}	the tensile failure of the beam-bottom
	L_{A2}	the tensile failure of the beam-bottom
	L_{A3}	the tensile failure of the beam-bottom
	PL_{B1}	the local compressive failure of the beam-end
	PL_{B2}	the horizontal joint failure
	PL_{B3}	the horizontal joint failure
	$PL_{C1\text{-}1}$	the horizontal joint failure
	$PL_{C2\text{-}1}$	the local compressive failure of the beam-end
	$PL_{C3\text{-}1}$	the local compressive failure of the beam-end
	$YL_{D1\text{-}1}$	the local compressive failure of the beam-end
	$YL_{D2\text{-}1}$	the local compressive failure of the beam-end
Regulated beams	$PL_{C1\text{-}2}$	the horizontal joint failure
	$PL_{C2\text{-}2}$	the local compressive failure of the beam-end
	$PL_{C3\text{-}2}$	the horizontal joint failure
	$YL_{D1\text{-}2}$	the local compressive failure of the beam-end
	$YL_{D2\text{-}2}$	the horizontal joint failure

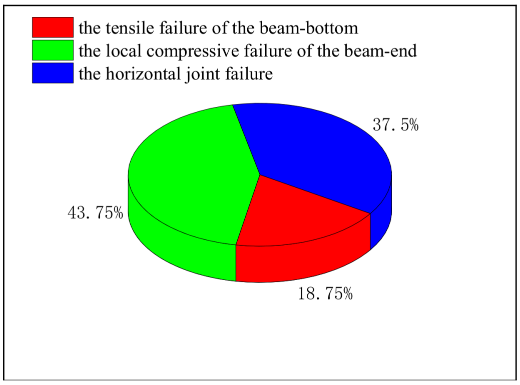

Figure 7. The distribution of the failure mode.

4. Discussion

4.1. Analysis of the Ultimate Load of Beams

To evaluate the influence of the creep and prestressed control on the mechanical properties of glulam beams, the ultimate load of the creep beams and the regulated beams were compared with that of the glulam beams. The glulam beams were absolutely identical to those used in former work and were directly subjected to short-term loading (see Table 5). For convenience, the glulam beam, which was directly under short-term loading, was named short-term beam below.

Table 5. Comparison of the ultimate load of creep beams and short-term beams.

Number of the Component	Ultimate Load (kN)	Percentage (%)
L_1 [1]	23.30	—
L_{A1}	27.09	16.3
L_{A2}	22.55	−3.2
L_{A3}	21.01	−9.8
PL_1 [1]	30.40	—
PL_{B1}	29.90	−1.6
PL_{B2}	27.92	−8.2
PL_{B3}	26.38	−13.2
PL_1 [1]	30.40	—
$PL_{C1\text{-}1}$	27.92	−8.2
PL_2 [1]	30.30	—
$PL_{C2\text{-}1}$	26.89	−11.3
PL_3 [1]	30.00	—
$PL_{C3\text{-}1}$	27.14	−9.5
YL_1 [1]	30.60	—
$YL_{D1\text{-}1}$	29.71	−2.9
YL_2 [1]	33.50	—
$YL_{D2\text{-}1}$	30.43	−9.2

[1] The beams L_i, PL_i, and YL_i in the table are short-term beams. Their values are the average of the short-term test results conducted by the research group in the early stage. The percentage of change is also compared with this standard. A positive value indicates an increase, and a negative value indicates a decrease.

It can be seen from Table 5 that after the long-term loading test, except for L_{A1}, the ultimate load of the reinforced glulam beam decreased. In the ordinary glulam beam test group (group of L_A), the ultimate load of the beam decreased with the increase in the long-term loading level. Compared with the short-term beam, the ultimate load of L_{A1} increased by 16.3%, while the ultimate load of L_{A2} and L_{A3} decreased 3.2% and 9.8%, respectively. The ultimate load of the L_{A1} beams was higher than that of the short-term beams because the bearing capacity of ordinary glulam beams was affected by glulam defects, and the dispersion was greater, while L_{A1} beams had fewer defects and lower long-term load, so the ultimate load was larger.

In the reinforced glulam beam group, compared with the short-term beam, the ultimate load decreased by 1.6–13.2%, and as the loading level increased, the ultimate load decreased more.

In the prestressed glulam beam group, compared with the short-term beams, the ultimate load of the PL_C group beams was reduced by 8.2–11.3% and the reinforcement ratio had little effect on the reduction of the beam ultimate load; the ultimate load of the YL_D group beams was reduced by 2.9–9.2%, as the prestress value of the beam increased, the limit load decreased more. This was because the greater the prestress applied to the beam, the greater the creep of the glulam, and therefore, the greater the impact on the bearing capacity of the beam.

In order to evaluate the influence of the prestress control on the mechanical performance of the beam, the ultimate load of the control beam was compared with the short-term beam under the same working conditions in the early stage of the research group, as shown in Table 6.

Table 6. Comparison of ultimate load of regulated beams, and short-term beams.

Number of the Component	Ultimate Load (kN)	Percentage (%)
PL_1	30.40	—
$PL_{C1\text{-}2}$	34.68	14.1
PL_2	30.30	—
$PL_{C2\text{-}2}$	31.70	4.6
PL_3	30.00	—
$PL_{C3\text{-}2}$	33.55	11.8
YL_1	30.60	—
$YL_{D1\text{-}2}$	32.61	6.6
YL_2	33.50	—
$YL_{D2\text{-}2}$	31.83	−5.0

It can be seen from Table 6 that compared with short-term beams, except for $YL_{D2\text{-}2}$ beam, the load-bearing capacity of control beams improved. The PL_C beams increased by 4.6–14.1%; $YL_{D1\text{-}2}$ beam increased by 6.6%.

In the reinforced glulam beam group the ultimate load of the regulated beam was improved. This was because, under the condition of maintaining the long-term loading value unchanged, the prestress was used to restore the initial deflection value of the beam to the loading state, which offset the deflection of the beam due to creep. Meanwhile, the distribution of the stress on the beam changed, and the height of the cross-section neutral axis was thus reduced. Since the height of the compression zone was greater, the failure mode of the beam experiences shifted from tensile failure to compressive failure. Therefore, the bearing capacity of the beam increased correspondingly.

In the prestressed glulam beam group, the ultimate load of the $YL_{D2\text{-}2}$ was reduced by 5.0%. This was because a large prestress was applied to the beam before the long-term loading. In the regulation process, the prestress was continuously applied so that the local pressure at the end of the beam was too large, resulting in the splitting of the glulam. In the loading process, the endplate prematurely lost the anchoring effect, reducing the bearing capacity of the beam. Therefore, in the actual project, the beam-end anchoring device should be further optimized to make the beam-end local pressure distribution more uniform. At the same time, the size of the prestress should be controlled to avoid beam-end local pressure damage.

4.2. Load-Deflection Curves

When comparing the load-deflection curves of the creep beam and the short-term beam under the same working conditions performed by the research group in the early stage, as shown in Figure 8, and stipulating that the initial mid-span deflection value of the beam was zero, the deflection downward was positive, inverted if negative.

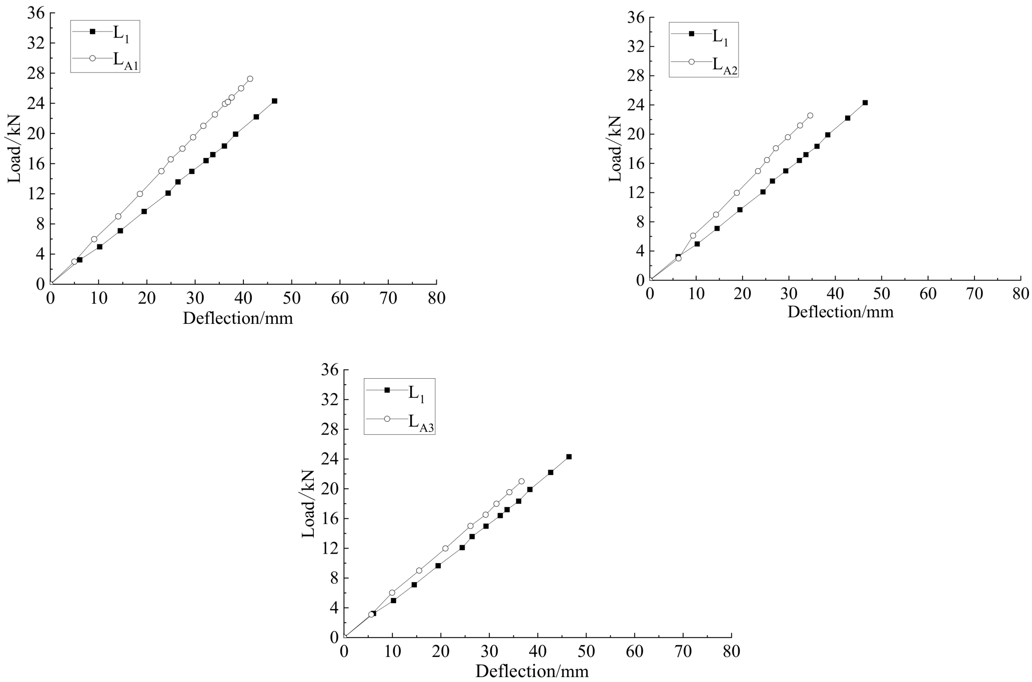

(**a**)

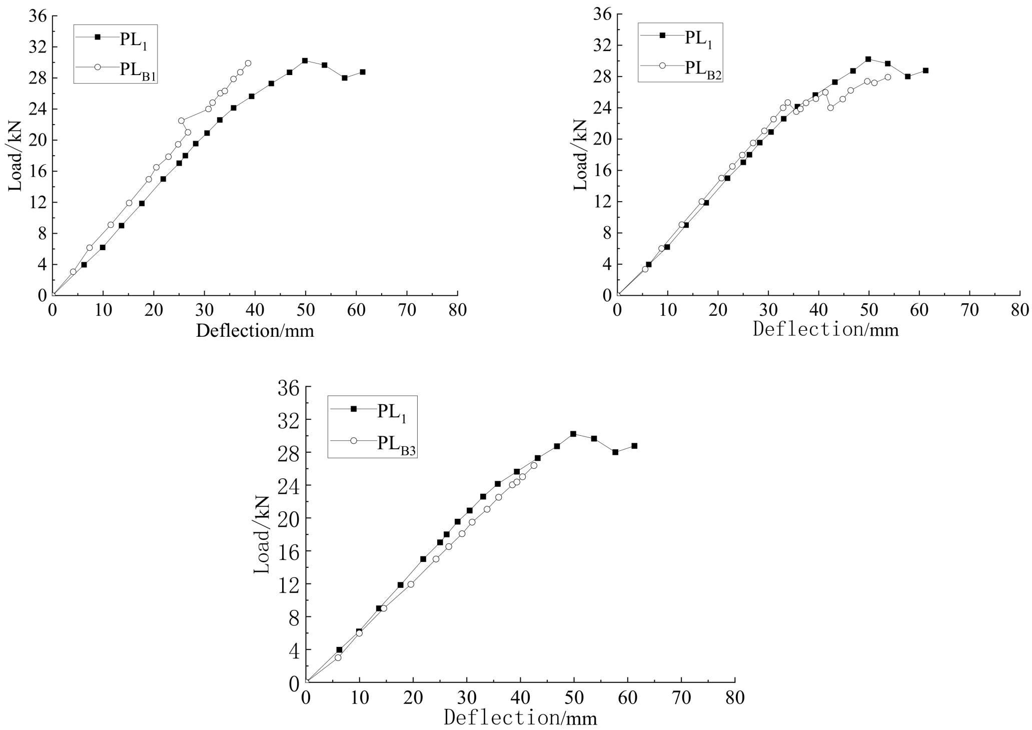

(**b**)

Figure 8. *Cont.*

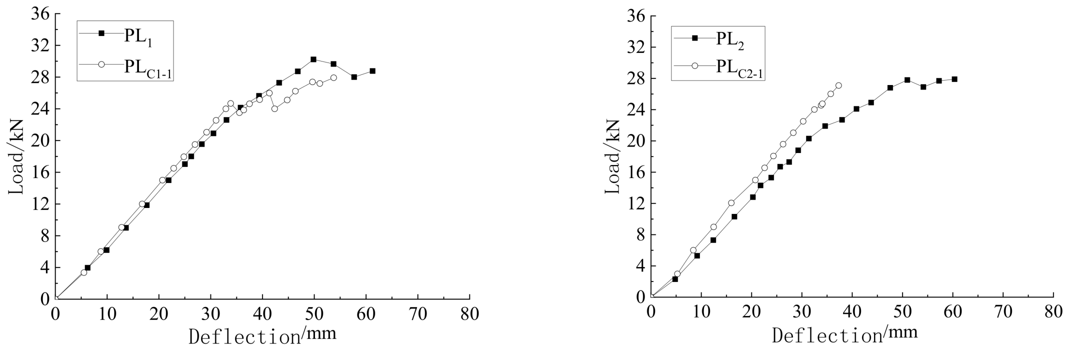

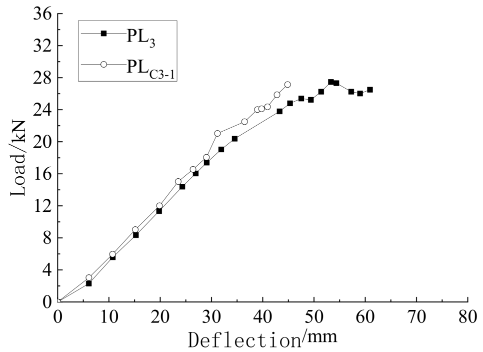

(**c**)

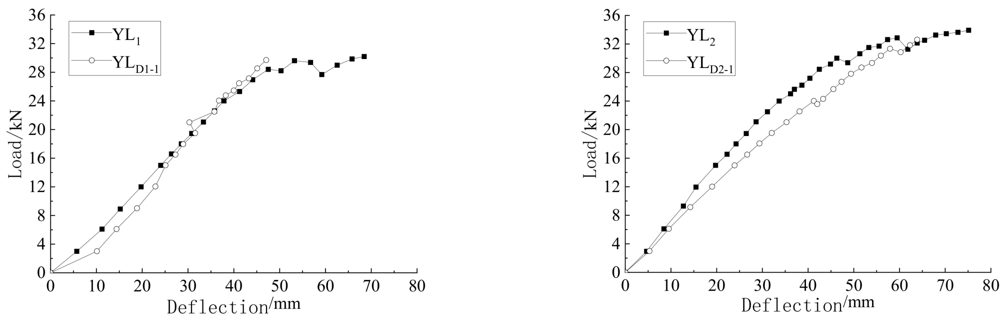

(**d**)

Figure 8. Load-deflection curves of creep beams and short-term beams. (**a**) The ordinary glulam beam (Group A); (**b**) the reinforced glulam beam (Group B); (**c**) the reinforced glulam beam (Group C); (**d**) the prestressed glulam beam (Group D).

It can be seen from Figure 8 that the change law of the load-deflection curves of the L_A, the PL_B, and the PL_C was roughly the same as that of the short-term beams. After the long-term loading test, the rigidity and ductility of the glulam beams were not affected too much. However, the bearing capacity and ultimate deflection of the creep beams were slightly reduced. The load-deflection curves of the YL_D group of beams were located below the short-term beams because the prestressed beams had obvious creeping changes in glulam, which led to a decrease in stiffness.

The load-deflection curves of the regulated beams and the short-term beams are shown in Figure 9. After the prestress control was performed, the slope of the load-deflection curves of the beam was greater than that of the short-term beam, which was more obvious for the YL_D group prestress, indicating that the stiffness of the beam increased after control and exceeded the short-term beam. The reason was the application of additional prestresses in the process of regulation. This process increased the tensile stress in the steel bar and the compressive stress in the glulam, which essentially increased the combined force of the two. The tension and compression force were coupled with the lever arm, so the stiffness of the beam was increased, but the excessive tensile stress in the control steel bar in the future made the beam-end local compression or horizontal joint failure, so the bearing capacity and ductility of the control beam were different declines.

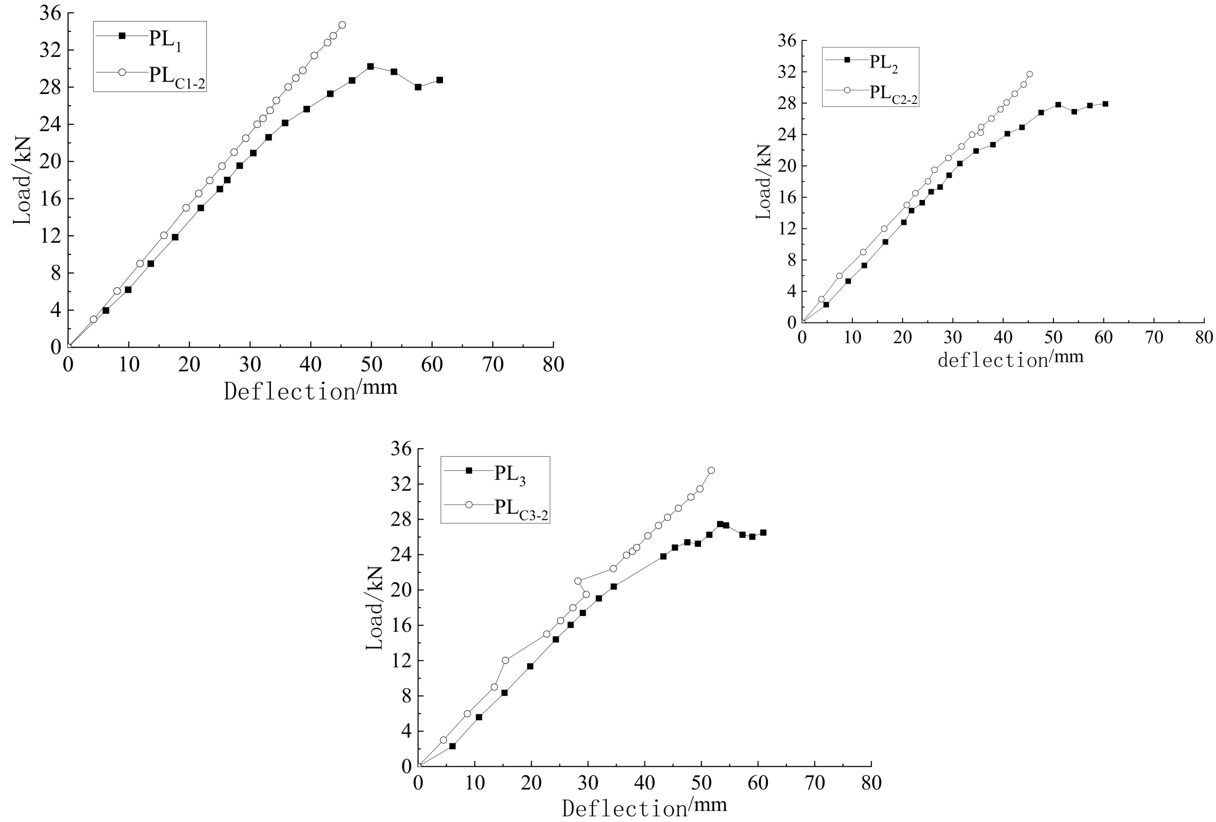

(**a**)

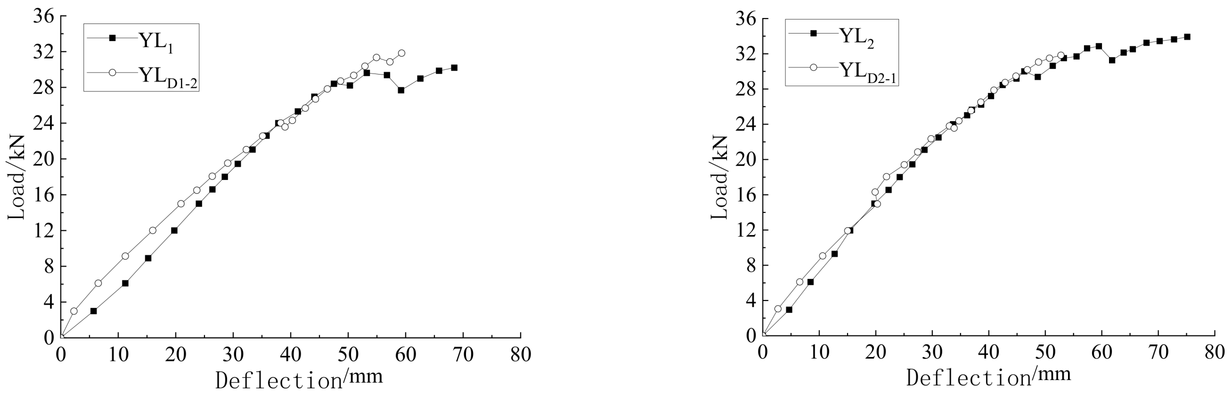

(**b**)

Figure 9. Load-deflection curves of regulated beams and short-term beams. (**a**) The reinforced glulam beam (Group C); (**b**) the prestressed glulam beam (Group D).

5. Conclusions

(1) After long-term loading, the glulam beams used in this paper mainly had three failure modes: the tensile failure of the beam-bottom, the horizontal joint failure, and the local compressive failure of the beam-end. The probability of the three failures was 18.75%, 37.5%, and 43.75%, the glulam beam experienced the tensile failure of the beam-bottom, while the horizontal joint failure and the local compressive failure of the beam-end happened in the reinforced glulam beam and the prestressed glulam beam;

(2) The creep of glulam had a certain effect on the ultimate load of the adjustable reinforced glulam beam. The ultimate load of the creep beam and the short-term beam was compared, the ultimate load of the glulam beam was reduced by 3.2–9.8%; the reinforced glulam beam dropped by 1.6–13.2%; the prestressed glulam beam dropped by 2.9–9.2%;

(3) By comparing the bearing capacity of the regulated beam and the short-term beam, it was found that the reinforced glulam beam increased by 4.6–14.1%, and the prestressed glulam beam increased by 6.6%, except for the reduced bearing capacity of the $YL_{D2\text{-}2}$ beam due to local compression. Compared with short-term beams, the load-bearing capacity of creep beams under load failure decreased by 13.2%, while the load-bearing capacity of control beams was increased, with a maximum increase of 14.1%, indicating that the prestress control could increase the load-bearing capacity of the beams;

(4) When comparing the load-deflection curve of the creep beam with that of the short-term beam, it revealed that the ultimate bearing capacity and the ultimate deflection of the creep beam were reduced. After the prestress regulation, the stiffness of the beam increased, but its ductility decreased slightly.

Author Contributions: Conceptualization, N.G.; methodology, L.L.; software, L.L.; formal analysis, G.L.; resources, Y.Z.; data curation, C.Y.; writing—original draft preparation, C.Y.; writing—review and editing, N.G.; funding acquisition, N.G. and G.L. and Y.Z. All authors have read and agreed to the published version of the manuscript.

Funding: This research work was supported by the Fundamental Research Funds for the Central Universities (2572017DB02), the natural science foundation of the Heilongjiang Province (LH2019E005), and the natural science of the Heilongjiang Province (LH2020E009), Funded by the Natural Science Foundation of the Fujian Province (2020J01402), Harbin science and technology innovation talent fund project (2017RAQXJ086).

Institutional Review Board Statement: Not applicable.

Informed Consent Statement: Not applicable.

Data Availability Statement: All the data were measured by experiments.

Conflicts of Interest: The authors declare that they have no conflicts of interest to report regarding the present study.

References

1. Kolb, J. *Multi-Storey Timber Structure*; Birkhäuser: Basel, Switzerland, 2008; pp. 188–200.
2. Kohler, J.; Svensson, S. Probabilistic representation of duration of load effects in timber structures. *Eng. Struct.* **2011**, *33*, 462–467. [CrossRef]
3. Wang, Z.; Li, H.; Lorenzo, R.; Corbi, I.; Corbi, O.; Fang, C. Review on bond properties between wood and fiber reinforced polymer. *J. Renew. Mater.* **2020**, *8*, 993–1018. [CrossRef]
4. Lam, E. Tall Wood Buildings: Design, Construction and Performance. In *Canadian CLT Handbook*, 2019th ed.; National Library of Canada: Ottawa, ON, Canada, 2020; Volume 65, pp. 48–49.
5. Viholainen, N.; Kylkilahti, E.; Autio, M.; Toppinen, A. A home made of wood: Consumer experiences of wooden building materials. *Int. J. Consum. Stud.* **2020**, *44*, 542–551. [CrossRef]
6. Sassu, M.; de Falco, A.; Giresini, L.; Puppio, M.L. Structural Solutions for Low-Cost Bamboo Frames: Experimental Tests and Constructive Assessments. *Materials* **2016**, *9*, 346. [CrossRef]
7. Lu, W.; Song, E.; Yue, K.; Liu, W. Experimental study on creep performance of FRP board reinforced glued-wood beam. *Build. Mater.* **2013**, *16*, 294–297.
8. He, M.; Lu, W.; Yue, K.; Song, E. FRP enhances creep property of glue-wood arch. *J. Nanjing Univ. Technol.* **2013**, *35*, 107–110.
9. Zuo, H.; Li, Y.; Fu, D.; Guo, N. Influence of size effect on bending performance of reinforced glulam beams. *J. Northeast For. Univ.* **2019**, *47*, 62–65.
10. Yang, H.; Liu, W.; Lu, W.; Zhu, S.; Geng, Q. Flexural behavior of FRP and steel reinforced glulam beams: Experimental and theoretical evaluation. *Constr. Build. Mater.* **2016**, *106*, 550–563. [CrossRef]
11. Soriano, J.; Pellis, B.P.; Mascia, N.T. Mechanical performance of glued-laminated timber beams symmetrically reinforced with steel bars. *Compos. Struct.* **2016**, *150*, 200–207. [CrossRef]
12. Daniel, L.; Ghasan, D. Towards enhancing the post-peak performance of glued-laminated timber beams using multi-directional fibre reinforced polymers. *Eng. Struct.* **2020**, *215*, 110680.

13. Yang, H.; Ju, D.; Liu, W.; Lu, W. Prestressed glulam beams reinforced with CFRP bars. *Constr. Build. Mater.* **2016**, *109*, 73–83. [CrossRef]
14. Zhu, E.; Zhou, H. Creep Buckling of Laminate Arch. *J. Shenyang Jianzhu Univ.* **2009**, *25*, 640–655.
15. Akbarzadeh, I.; SattariFar, I.; Salehi, M. Numerical and experimental study of the effect of short-term and long-term creep modeling in stress relaxation of a multi-pass welded austenitic stainless steel pipe. *Mater. Sci. Eng. A* **2010**, *528*, 2118–2127. [CrossRef]
16. He, T. The Study on Flexural Performance of Prestressed Glulam Beams Based on the Creep Behavior. Master's Thesis, Northeast Forestry University, Harbin, China, 2016.
17. Chen, H. The Study on Flexural Performance of Regulable Reinforcement Glulam Beams Based on the Creep Behavior. Master's Thesis, Northeast Forestry University, Harbin, China, 2017.
18. Thelandersson, S.; Larsen, J.H. *Timber Engineering*; John Willey & Sons Ltd.: Hoboken, NJ, USA, 2003; pp. 131–152.
19. Corbi, I.; Corbi, O.; Li, H. A coupled control strategy for the mitigation of structural vibrations. *Ing. Sismica* **2019**, *36*, 107–117.
20. Guo, N.; Xiong, H.; Wu, M.; Zuo, H.; Jiang, F.; Hou, X.; Xin, D. Long-Term Bending Behaviour of Prestressed Glulam Bamboo-Wood Beam Based on Creep Effect. *Struct. Durab. Health Monit.* **2020**, *14*, 229–248. [CrossRef]
21. Liu, Q.; Yang, H. Experimental study on flexural behavior of Engineering timber beams. *J. Build. Struct.* **2008**, *29*, 90–95.
22. Ribeiro, A.S.; de Jesus, A.M.P.; Lima, A.M.; Lousada, J.L.C. Study of strengthening solutions for glued-laminated wood beams of maritime pine wood. *Constr. Build. Mater.* **2009**, *23*, 2738–2745. [CrossRef]
23. Sun, X.; Liu, W.; Lu, W.; Zhu, X.; Yuan, S. Study on bending performance test and engineering application of glued-wood string beam. *J. Nanjing Univ. Technol.* **2016**, *38*, 121–128.
24. Zuo, H.; Di, J.; Wang, T. Lateral resistance of shear wall of light timber structure with prestressed cross tie bar under low cyclic reciprocating load. *J. Northeast For. Univ.* **2019**, *47*, 61–64.
25. Zuo, H.; Liu, H.; Lu, J. The effect of new self-tapping screw reinforcement measures on the bending performance of glued timber beams. *J. Northeast For. Univ.* **2020**, *48*, 112–116.
26. *Standard for Design of Timber Structures*; GB50005-2017; Ministry of Housing and Urban-Rural Development of the People's Republic of China (MOHURD): Beijing, China; General Administration of Quality Supervision, Inspection and Quarantine of the People's Republic of China (AQSIQ): Beijing, China, 2017.
27. CSA Group. *Engineering Design in Wood (086-14)*; CSA Group: Toronto, ON, Canada, 2017; ISBN 978-1-77139-448-2.